Large Off-Diagonal Contribution to the Second-Order Optical Nonlinearities of Λ-Shaped Molecules

Mingli Yang and Benoît Champagne*

Laboratoire de Chimie Théorique Appliquée, Facultés Universitaires Notre-Dame de la Paix, B-5000 Namur, Belgium

Received: October 20, 2002; In Final Form: February 20, 2003

The diagonal and off-diagonal tensor components of the first hyperpolarizability of a series of Λ-shaped molecules are compared by means of ab initio and semiempirical molecular orbital calculations. The calculated results are rationalized using expressions derived from a simple valence-bond charge-transfer model in which one ground and two excited state are described as a combination of one valence-bond (VB) and two charge-transfer (CT) states. In addition to the CT character, the angle (2θ) between the two donor (D)/acceptor (A) branches is a key parameter to determine the relative magnitudes between the β_{xxz} and β_{zzz} components. In the VB-2CT model, β_{xxz} presents a maximum value for $2\theta = 109.47°$, whereas β_{xxz} and μ_z have the same sign. On the other hand, β_{zzz} decreases monotonically with θ, and its variations with the CT character follow a curve with two extrema like for one-dimensional D/A chromophores. The ab initio and semiempirical calculations as well as the VB-2CT model show that Λ-shaped molecules with large first hyperpolarizability and specific $\eta = \beta_{xxz}/\beta_{zzz}$ can be designed in order to build phase-matchable second-harmonic generation crystals.

1. Introduction

Second-order nonlinear optical (NLO) materials have attracted much interest because of their potential applications in optoelectronic technology.[1−3] Typical second-order NLO chromophores are one-dimensional π-conjugated systems end-capped with donor (D) and acceptor (A) moieties. A great deal of theoretical and experimental works have been carried out over the past two decades toward a comprehensive understanding of the structure−property relationships:[2−6] Significant molecular hyperpolarizabilities β can be achieved by optimizing the D/A strengths and/or extending the conjugation path.

However, some apparent problems exist in the NLO properties of these 1-D compounds. One is the transparency−efficiency tradeoff, which is difficult to settle with conventional D/A systems because the desirable increase in β is accompanied by a bathochromatic shift of the electronic transition.[2,7,8] Moreover, most one-dimensional push−pull molecules favor the formation of centrosymmetric arrangement in crystal because of the dipole−dipole intermolecular interaction and exhibit no second-harmonic generation (SHG) response. Another problem concerns the phase-matching conditions;[9,10] that is, an optimal molecular orientation in the crystal is essential to obtain efficient phase-matched SHG. For the *1*, *2*, *m*, and *mm2* crystal point groups, the optimal angle between the molecular charge transfer (CT) axis (chosen generally to be the *z* axis) and the crystal principal dielectric axis is predicted as 54.7° (or 125.3°) in the case of one-dimensional push−pull molecules for which only one molecular β-tensor component, β_{zzz}, is assumed to be nonnegligible. Unfortunately, as shown by Zyss and Oudar,[11] who determined the relationships between microscopic (molecular) and macroscopic (crystal) nonlinearities, such an orientation allows only to recover, at the macroscopic scale, 38% of the microscopic response. For higher symmetry crystals, the effective phase-matched nonlinearities are even smaller, whereas other factors also influence the macroscopic NLO responses.[12] This is why compounds with large off-diagonal β-tensor components appear as relevant alternatives to display large macroscopic NLO responses.

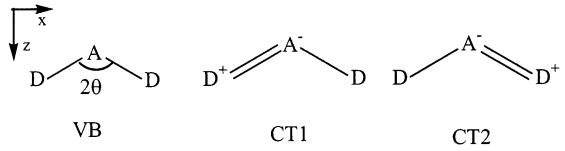

Figure 1. Resonant forms of a Λ-shaped molecule.

Beyond the classical one-dimensional dipolar systems, a new concept based on molecules with two- or three-dimensional geometries has been proposed.[13] Octupolar molecules such as 1,3,5-triamino-2,4,6-trinitrobenzene (TATB) are typical examples that exhibit second-order NLO responses as large as their dipolar analogues.[14] These nondipolar chromophores are regarded as promising NLO candidates because of their improved nonlinearity/transparency tradeoff and because of the possibility of noncentrosymmetric arrangements owing to the lack of a permanent dipole moment. Moreover, these two-dimensional chromophores have been observed to possess better phase-matching than one-dimensional chromophores because of their larger off-diagonal components.[9,10,15]

Besides octupolar systems, significant NLO responses have also been observed in two-dimensional Λ-shape molecules[16−23] where the two D/A pairs intersect at the donor or acceptor group constituting a DAD- or ADA-like structure (Figure 1). In such compounds, there are two CT axes, and the angle they form is defined as 2θ. These Λ-shaped molecules have been reported to form transparent and phase-matchable noncentrosymmetric crystal structures that can exhibit large second-order NLO responses owing to the large off-diagonal β-tensor component.[16−23] In recent years, much interest has also been paid

* To whom correspondence should be addressed.

10.1021/jp0272567 CCC: $25.00
Published on Web 04/15/2003

to organometallic and coordination compounds among which the dipolar two- and three-dimensional metal complexes which turn out to be very promising candidates for NLO applications.[24−26] In addition to improved phase-matching behavior and noncentrosymmetric crystal packing, thermal stability has also been reported for two-dimensional organic compounds.[27]

This theoretical investigation aims at deducing structure−property relationships between the diagonal and off-diagonal first hyperpolarizability tensor components in Λ-shaped molecules. This is performed in three steps: (i) semiempirical and ab initio quantum chemical approaches are employed to calculate the β-tensor components of model systems as well as of Λ-shaped molecules that have already been characterized experimentally, (ii) a one-valence-bond two-charge-transfer (VB-2CT) model is introduced and applied to determine the key factors that influence the diagonal and off-diagonal first hyperpolarizability tensor components of Λ-shaped molecules, and (iii) the VB-2CT model is employed to further explain the trends observed in the calculated semiempirical and ab initio data.

VB−CT models, which were first proposed by Mulliken[28] for investigating structural and spectral properties of molecular D/A complexes, have long been used to provide both qualitative and quantitative descriptions of physicochemical phenomena. They already met some success in predicting structure−property relationships for the electronic hyperpolarizabilities of push−pull dipolar chromophores[29−33] but not for their extension to vibrational hyperpolarizabilities which remains questionable in what concerns the ratios between the electronic and vibrational counterparts.[34−38] This is however not a problem in this study which focuses on the SHG response because, compared to the zero-point averaging correction, the vibrational SHG contribution is negligible.[6] For Λ-shaped molecules, a VB-2CT model is adopted because of the limitation of the two-state VB−CT approximation in dealing with hyperpolarizabilities of systems possessing two donors or two acceptors. Similar variations of VB−CT models have been developed for various systems in which additional higher excited states contribute to the NLO responses. Cho et al.[39−41] have proposed one-valence-bond two-charge-transfer (VB-2CT) and one-valence-bond three-charge-transfer (VB-3CT) models for quadrupolar and octupolar molecules, respectively. More recently, Barzoukas and Blanchard-Desce[42] have presented a three-form three-state model to tackle the two-photon absorption of dipolar and quadrupolar molecules, whereas Cho et al.[43] elaborated a five-state model to describe the NLO properties of tetrahedral donor−acceptor octupolar molecules.

Section 2 outlines the computational strategy for calculating the β components of Λ-shaped molecules. The calculated results are presented and discussed in section 3. In section 4, the VB-2CT expressions for individual β components as well as related quantities (CT character, dipole moment, dipole transition moments, and excitation energies) are derived and characterized. Then they are used to interpret the semiempirical and ab initio calculations.

2. Compounds and Computational Methodology

The Λ-shaped molecules with DAD or ADA patterns, drawn in Figure 2, are chosen as prototypes or as reference compounds to address the correlation between the diagonal and off-diagonal β-tensor components. A1 and A2 are homologues in which the carbonyl group acts as an acceptor and the amino or *N*,*N*-dimethylamino moieties as donors. B1, B2, and B3 are *meta*-di-amino-, *meta*-hydroxy-, *meta*-fluoro-benzenes, respectively,

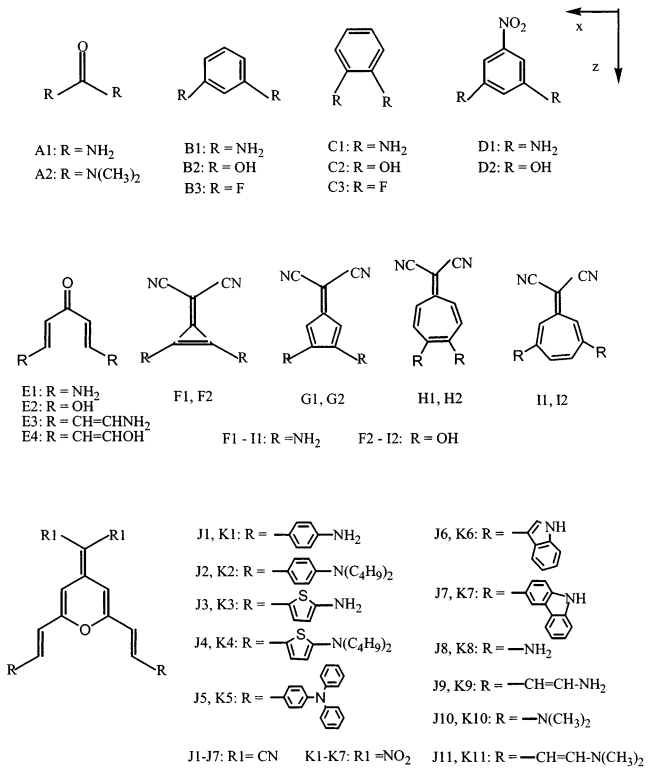

Figure 2. Λ-shaped molecules with donor−acceptor-donor or acceptor−donor−acceptor patterns.

whereas C1, C2, and C3 are the corresponding *ortho*-disubstituted isomers. With respect to the phenyl group, these substituents are π donors and σ acceptors,[44] and therefore, the global effect will result from their relative importance. D1 and D2 are DAD molecules in which the strong electron acceptor (NO_2 group) interacts with the amino- or hydroxy-donor groups. This interaction is however relatively weak because the D/A pairs are in the *meta* position. Other structures are also proposed to sample the different CT domains including structure E where the conjugated linker is longer than in urea as well as cyclic compounds (F−I) which display different values for the 2θ angle. The CT directions in the E−I groups are not as obvious as those in the A−E groups where the 2θ angle is about 60° or 120°. In the E−I groups, 2θ is defined by the line passing through the heteroatom of the π donor and the carbon atom connecting either the cyano groups for the F−I molecules or the oxygen atoms for the E molecules.

The angle between the two D−A branches is about 120° for A1, A2, B1, B2, B3, D1, and D2, about 90° for the E systems, and about 60° for C1, C2, and C3 as well as for three-membered rings (F1 and F2). In the five-membered rings, the angle between the CT axes is slightly larger than 30°, whereas for the seven-membered rings, the angle ranges from 24 to 27° to 76−77° when donor groups are in 2,5 and 3,4 positions, respectively. In addition to the charges, one parameter to assess the amount of charge transfer in the ground state is the geometry and in particular the bond length alternation (BLA) of the carbon backbone. For instance, in D/A polyenes when increasing the strength of the D/A pair, and therefore when increasing the charge transfer from the D to the A, the BLA decreases to reach zero in the cyanine limit, and then it changes sign and increases in magnitude.[2,6] When the compound contains rings, aromaticity effects also play a role in favoring or unfavoring bond length equalization. For the compounds of the B−D groups, the geometry of the ring is little changed by the presence of donors

and/or acceptors (BLA ≤ 0.01 Å) so that they belong to the category of compounds where the ground-state electronic structure is dominated by the VB form. On the other hand, in the A and E groups, the CT character is larger but the molecules still present a polyenic structure and an important BLA (0.09−0.12 Å). The structures with three- and seven-membered rings present smaller BLA than the five-membered ring compounds. Indeed, for the F1, H1, and I1 compounds, the (average) BLA amounts to 0.039, 0.046, and 0.040 Å, respectively, whereas it reaches 0.082 Å in G1. When replacing the amino group by a weaker donor (the hydroxy group), the BLA increases and is, in the same order, 0.060, 0.050, 0.055, and 0.095 Å. The distinction between the three- and seven-membered rings and the five-membered rings is related to the tendancy of the three- and seven-membered rings to give an electron, whereas the five-membered rings tend to monopolize one more electron in order to form an aromatic entity.

Group J consists of a series of (dicyanomethylene)pyran chromophores exhibiting high optical nonlinearities and for which the red shifts associated with chemical substitutions are smaller than in most other classes of chromophores but lead to larger β.[17] In addition to the chromophores of ref 17, the J8-J11 molecules which contain a polyenic segment are also considered. Group K is obtained by substituting the cyano moieties of group E by nitro moieties that possess a stronger π-acceptor character.[44] The backbone of these molecules lies in the *xz* plane with the *z* axis passing through their 2-fold axis (or approximate 2-fold axis). Most of the molecules of J and K groups present a valence bond form. However, the molecules with the stronger acceptor (NO_2) and the smaller polyenic segment (K8, K10) display the smallest BLA (0.06−0.07 Å) and are close to the cyanine limit.

Because of their large size, molecules of groups J and K are treated at the AM1[45] semiempirical level, whereas the A−I systems are investigated ab initio. The geometry optimizations were performed at different levels of approximation (HF/6-311G** for A−D and MP2/6-31G** for E−I), whereas electron correlation has been included in computing the first hyperpolarizability and dipole moment. This has been carried out by adopting the numerical finite field (FF) procedure[46] within the Møller−Plesset second-order scheme (MP2) (frozen-core approximation). In this approach, the dipole moment and first hyperpolarizability tensor components are given by the (opposite of the) first and third derivatives of the field-dependent energy with respect to the external electric field. The various finite difference expressions are given in ref 47. The numerical errors have been reduced by using a tight (10^{-11} a.u.) threshold on the SCF energy as well as by adopting the Romberg procedure[48] to eliminate the higher-order contaminations. Field amplitudes of 2^kF with $F = 0.0008$ and k ranging between 0 and 3 have been used to attain an accuracy of 1−10 au on the β-tensor components. By relying on our experience on the interplay between the size of the atomic basis set and the accuracy of the calculations,[6,49,50] the 6-31+G(d) basis set which contains one set of polarization functions and diffuse functions has been chosen to ensure semiquantitative accuracy of our estimates. Only static properties have been evaluated at this level of theory. All ab initio calculations have been performed using Gaussian 98.[51]

The AM1 parametrization[45] with the "precise" option of the MOPAC 2000 package[52] has been used for optimizing the molecular geometry of the J and K molecules. The first hyperpolarizability tensor components have been evaluated at the time-dependent Hartree−Fock (TDHF) level[53] with a cutoff tolerance of 0.001 au. Both static and dynamic quantities are reported. The SHG values have been determined for wavelengths of 1907 and 1064 nm.

TABLE 1: Calculated Dipole Moment and Static First Hyperpolarizability Tensor Components of Λ-Shaped Molecules in Comparison with the 2θ Angle[a]

molecules	μ_z	β_{xxz}	β_{yyz}	β_{zzz}	2θ	η^b	$\beta_z{}^c$	$\beta_z{}'^d$
A1	1.43	54	−26	−40	114	−1.37	−11	14
A2	1.26	91	−5	−85	116	−1.07	1	6
B1	0.36	310	42	35	121	8.97	386	344
B2[e]	−1.01	−218	−63	−38	116	5.74	−320	−256
B3	−0.61	−124	−43	−21	120	5.89	−188	−145
C1	0.31	110	56	362	56	0.30	528	472
C2[e]	−0.60	−99	−97	−307	60	0.32	−503	−406
C3	−1.05	−61	−73	−202	59	0.30	−336	−263
D1	2.19	274	−39	269	120	1.02	504	543
D2[e]	2.68	173	16	170	124	1.02	360	344
E1	2.36	534	21	267	96	2.00	822	801
E2	2.63	333	0	235	95	1.42	568	568
E3	2.97	1945	21	1153	87	1.68	3118	3098
E4	1.28	1304	0	863	87	1.51	2167	2167
F1	4.47	374	−19	−54	60	−6.93	301	320
F2	4.57	282	10	107	61	2.64	399	389
G1	4.12	537	−40	2221	35	0.24	2718	2758
G2	1.84	236	35	1569	33	0.15	1840	1805
H1	5.27	696	−152	2302	27	0.30	2846	2998
H2	3.03	566	5	2181	24	0.26	2752	2747
I1	4.64	1277	−76	−671	76	−1.90	530	606
I2	4.72	725	−25	579	77	1.25	1279	1304

[a] The μ and β values are evaluated at MP2/6-31+G(d) level. All quantities are in au (1.0 au of dipole moment = 8.478 358 × 10^{-30} Cm = 2.5415 D; 1.0 au of first hyperpolarizability = 3.2063 × $10^{-53}C^3m^3J^{-2}$ = 8.641 × 10^{-33} esu). [b] $\eta = \beta_{xxz}/\beta_{zzz}$. [c] $\beta_z = \beta_{xxz} + \beta_{zzz} + \beta_{yyz}$. [d] $\beta_z' = \beta_{xxz} + \beta_{zzz}$. [e] (*Z*,*Z*) conformation.

3. Computational Results

Tables 1 and 2 list the calculated dipole moments and first hyperpolarizabilities of all the molecules shown in Figure 2. Generally speaking, the dipole moment of such molecules is determined by the D/A strengths: the stronger the D/A pair, the larger the dipole moment. In addition, it is also determined by the charge distributions in the whole molecule and both the inductive (σ) and mesomer (π) effects contribute whereas the variations of the first hyperpolarizability are generally dominated by π-electron effects.[54] This can explain why A2, which has stronger donors, possesses a smaller dipole moment than A1. Similarly, the variations of μ_z in the B and C groups can be explained by the increase of the σ-acceptor character in the NH_2, OH, and F series while the π-donor character decreases.

For a molecule with C_{2v} symmetry, there are only three nonzero β-tensor components, β_{xxz}, β_{yyz}, and β_{zzz}. B2, B3, C2, C3, and D2 are found to possess C_{2v} symmetry, whereas the symmetry is broken by the out-of-plane amine or methyl groups in the other molecules. As a result, some β components, which strictly vanish for a C_{2v} symmetric molecule, become nonzero. However, because these molecules keep roughly the C_{2v} symmetry, these nonzero components are too small so that the following discussion is only concerned with the β_{xxz}, β_{yyz}, and β_{zzz} components. Because the molecules lie in the *xz* plane, the β_{xxz} and/or β_{zzz} components are usually larger than the corresponding β_{yyz} values. The β_{xxz} and β_{zzz} components are comparable in magnitude for each molecule of the A and D groups, but larger differences between the two components are found for the molecules of the B and C groups. β_{xxz} is much larger in absolute value than β_{zzz} for the molecules of B group, whereas a reverse situation is found for the molecules of the C group.

TABLE 2: Calculated Dipole Moment and SHG First-Order Hyperpolarizability Components of Λ-Shaped Molecules [a]

		$\omega = 0$					$\lambda = 1907$ nm, $\hbar\omega = 0.65$ eV					$\lambda = 1064$ nm, $\hbar\omega = 1.17$ eV							$\lambda = 1907$ nm
	μ_z	β_{xxz}	β_{yyz}	β_{zzz}	η[b]	$\beta_{\|\|}$[c]	β_{xxz}	β_{yyz}	β_{zzz}	η[b]	$\beta_{\|\|}$	β_{xxz}	β_{yyz}	β_{zzz}	η[b]	$\beta_{\|\|}$	2θ	μ (exp)	$\beta_{\|\|}$ (expt) [h]
J1	4.62 4.30[d]	64	0	20	3.2	51 88[d]	87	0	30	2.9	69	241	0	98	2.5	190	83		
J2	5.37	67	−1	22	3.0	62	91	−1	33	2.8	85	270	−2	125	2.2	266	97	4.96 ± 0.04[e] 3.82[f]	272 ± 3[e] 221[f]
J3	4.61	59	0	27	2.2	52	83	0	39	2.1	72	228	−1	116	2.0	196	72		
J4	5.84	89	−1	61	1.5	90	129	−1	92	1.4	131	554	−3	435	1.3	632	76	5.15 ± 0.04[e]	298 ± 18[e]
J5	3.44	133	−2	−2	−66	76	37	0	−4	−9.3	121	92	−1	−7	13	397	97	3.89 ± 0.08[e]	242 ± 4[e]
J6	5.37	58	−1	5	12	39	76	−1	13	5.8	73	217	−4	57	3.8	207	59	4.68 ± 0.04[e]	98 ± 5[e,g]
J7	4.62	69	−1	8	8.6	46	86	−5	13	6.6	101	240	−15	51	4.7	244	74	4.21 ± 0.04[e]	146 ± 5[e,g]
J8	5.12	27	0	−2	−13	15	36	−1	−1	−36	20	85	−1	5	17	44	55		
J9	5.56	47	0	26	1.8	44	64	0	38	1.7	59	173	−1	115	1.5	159	54		
J10	5.13	36	−1	4	9.0	24	48	−1	8	6.0	32	121	−3	30	4.0	78	55		
J11	5.60	61	−1	39	1.6	59	85	−1	58	1.5	83	248	−4	187	1.3	246	54		
K1	6.22	92	−1	24	3.8	69	128	−1	37	3.5	98	401	−2	144	2.8	342	83		
K2	6.67	134	−1	43	3.1	106	190	−1	66	2.9	153	657	−2	265	2.5	616	97		
K3	6.43	87	0	32	2.7	71	126	−1	50	2.5	105	493	−2	222	2.2	498	73		
K4	7.50	126	−1	60	2.1	111	188	−1	95	2.0	170	942	−4	527	1.8	139	76		
K5	5.05	184	−5	3	61	109	264	−7	11	24	164	1093	−22	118	9.3	854	98		
K6	7.08	81	−1	6	13	51	114	−2	15	7.6	75	373	−5	85	4.4	281	59		
K7	6.21	94	−2	11	8.5	67	131	−3	20	6.6	96	412	−13	92	4.5	338	74		
K8	6.85	35	−1	−11	−3.2	15	47	−1	−11	−4.3	20	126	−2	−16	−7.9	62	55		
K9	7.46	70	−1	24	2.9	56	98	−1	38	2.6	80	309	−3	141	2.2	287	55		
K10	6.98	49	−1	−5	−9.8	26	68	−2	−3	−23	37	194	−4	10	19	126	55		
K11	7.53	88	−2	41	2.1	77	126	−2	64	2.0	112	430	−5	244	1.8	458	55		

[a] The μ and β values are evaluated at the RHF/AM1 and TDHF/AM1 level, respectively. μ is given in au and β in 10^2au. [b] $\eta = \beta_{xxz}/\beta_{zzz}$. [c]

$$\beta_{||} = \frac{3}{5}\frac{\sum_i \mu_i \beta_i}{||\vec{\mu}||}, \text{ with } \beta_i = \sum_j \beta_{ijj},\ i, j = x, y, z.$$

[d] Reference 22. [e] EFISH measurements by Moylan et al. in chloroform.[17] [f] EFISH measurements by Ermer et al. in NMP.[55] [g] Experimental values for the N-hexyl substituted E6 or E7, whereas all of the calculations reported in this table are carried out with hydrogen atoms for simplicity. [h] After accounting for the difference of convention between theory and experiment as well as for the new quartz reference [Roberts, D. A. *IEEE J. Quantum Elec. QE* **1992**, *28*, 2057. Mito, A.; Hagimoto, K; Takahashi, C. *Nonlinear Opt.* **1995**, *13*, 3].

The angle between the two CT axes (2θ, see Figure 1) which is about 120° and 60° for B and C groups, respectively, appears as the key factor affecting the relative magnitude of these two components. Indeed, assuming that each D/A pair is characterized by a β_{aaa} value oriented along the D/A axis, a large angle tends to generate large off-diagonal component β_{xxz}, whereas a small angle tends to generate large diagonal β_{zzz}. Because inductive effects are rather important in these B−D systems owing to the absence of strong π acceptor (B and C groups) or to the weak conjugation between the donor and the acceptor (D group), changing the π donor or adding a π acceptor (nitro) can result in changes of both the sign and the magnitude of β, but in all cases, β remains small in comparison with other NLO systems such as *p*-nitroaniline or MNA.[2,6] Compared to the A systems, in the E systems, the conjugated path is larger, the 2θ angle is smaller, and both β_{xxz} and β_{zzz} have now the same sign.

The cyclic structures having small 2θ values (G and H groups) possess rather substantial β_{zzz} values and small $\eta = \beta_{xxz}/\beta_{zzz}$ ratio. When going from G1 to G2 or from H1 to H2, both the angle and η decrease, which therefore confirms the role of 2θ for explaining the variations in η. However, G1 (G2) possesses a larger 2θ angle than H1 (H2), whereas the β_{xxz}/β_{zzz} ratio is smaller. In F1 and F2, 2θ is very similar to the molecules of the C group but the β_{xxz} component is dominant. Moreover, the negative (positive) value of β_{zzz} occurs for the NH_2−(OH-)-substituted compound, whereas in C1 (C2), β_{zzz} is positive (negative). The situation is similar for the I1 and I2 compounds although the 2θ angle is larger than in F1−F2 and the amplitude of η decreases. These results show that large β_{xxz} and β_{zzz} values can be obtained with a broad range of η ratios and that 2θ is not the unique factor which influences them.

The large $\beta_{||}$ values of the molecules of the J and K groups, as listed in Table 2, are attributed to their large off-diagonal components which are always positive, whereas β_{zzz} can be either positive or negative. The geometry of these (dicyanomethylene)pyran chromophores is essentially planar except J2, J4, K2, and K4 in which the bulky butyl groups distort the molecular geometries. In these out-of-plane structures, other β components such as β_{xxx} are nonnegligible but small, and they are not reported here because this goes beyond the scope of this investigation. Although the variations of β in the J1−J7 and K1−K7 compounds are more or less consistent in what concerns the rule of thumb "large 2θ leads to large η", they also present some deviations. Replacing the cyano groups by stronger nitro groups leads to an increase in both β_{xxz} and β_{zzz} components with the exception of β_{zzz} in the J8-J11/K8−K11 compounds that possess the smallest BLA. Similarly, when going from NH_2 to $N(C_4H_9)_2$ and then to $N(Ph)_2$, the π-donor character increases leading to an increase of β_{xxz}, whereas the evolution of β_{zzz} is nonmonotonic. Substituting the aromatic linker by small polyenic segment leads to a reduction of β_{xxz} that can be associated to the smaller 2θ angles. For the longer segment, $(CH{=}CH)_2$, β_{zzz} is positive and 1.6 to 3.0 times smaller than β_{xxz}, whereas for the smaller linker, (CH═CH), the amplitude of β_{zzz} is much smaller while it can be either positive or negative. When moving from the static to the dynamic cases, most substitution effects on β_{xxz}, β_{zzz}, and their ratio are unchanged. The larger the frequency, the larger the β-tensor components. However, because β_{zzz} increases more than β_{xxz}, η decreases. The exceptions are the J8, J10, K8, and K10 compounds for which β_{zzz} is smaller and either positive or negative.

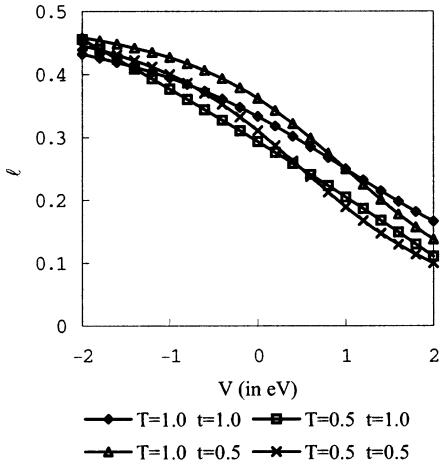

Figure 3. Charge-transfer character (ℓ) as a function of the energy gap between the CT and VB configurations ($V = E_C - E_V$) for different values of the resonance integrals (t and T).

4. VB-2CT Model

A typical Λ-shaped C_{2v} molecule can be modeled, as shown in Figure 1, by one VB and two CT forms. Within the VB-2CT model, the electronic wave functions of the ground and excited states are written as combinations of the limiting covalent and charge-transfer wave functions ϕ_{VB}, ϕ_{CT1}, and ϕ_{CT2}, respectively. The Hamiltonian matrix in the basis set of $\{\phi_{VB}, \phi_{CT1}, \phi_{CT2}\}$ is given by

$$H = \begin{pmatrix} E_V & -t & -t \\ -t & E_C & -T \\ -t & -T & E_C \end{pmatrix} \quad (1)$$

where E_V and E_C denote respectively the electronic energies of the VB and CT forms. $-t = \langle\phi_{VB}|H|\phi_{CT1}\rangle = \langle\phi_{VB}|H|\phi_{CT2}\rangle$ and $-T = \langle\phi_{CT1}|H|\phi_{CT2}\rangle$ are the transfer integrals between the VB and CT forms and between the two CT forms, respectively. The eigenvalues of this Hamiltonian (eq 1) are

$$E_0 = \frac{1}{2}(E_V + E_C - T) - \frac{1}{2}\sqrt{(V-T)^2 + 8t^2} \quad (2)$$

$$E_1 = E_C + T \quad (3)$$

$$E_2 = \frac{1}{2}(E_V + E_C - T) + \frac{1}{2}\sqrt{(V-T)^2 + 8t^2} \quad (4)$$

where $V = E_C - E_V$. The corresponding eigenfunctions are

$$\Psi_0 = \sin\delta\phi_{VB} + \frac{\sqrt{2}}{2}\cos\delta\phi_{CT1} + \frac{\sqrt{2}}{2}\cos\delta\phi_{CT2} \quad (5)$$

$$\Psi_1 = \frac{\sqrt{2}}{2}(\phi_{CT1} - \phi_{CT2}) \quad (6)$$

$$\Psi_2 = \cos\delta\phi_{VB} + \frac{\sqrt{2}}{2}\sin\delta\phi_{CT1} + \frac{\sqrt{2}}{2}\sin\delta\phi_{CT2} \quad (7)$$

where

$$\cos^2\delta = \frac{1}{2} - \frac{V-T}{2\sqrt{(V-T)^2 + 8t^2}} = 2\ell \quad (8)$$

The above formulas were first derived by Cho and co-workers[41] for assessing the second hyperpolarizability of centrosymmetric quadrupolar systems of which the first hyperpolarizability vanishes. Wolff and Wortmann[56] as well as Barzoukas and Blanchard-Desce[42] provided a similar treatment for the case where the coupling between the two CT forms is neglected, i.e., $T = 0$. Before deriving the expressions of the β-tensor components, we give a short description of the δ and ℓ characters. From eq 8, δ and ℓ are determined by the energy gap V between VB and CT states as well as by the transfer

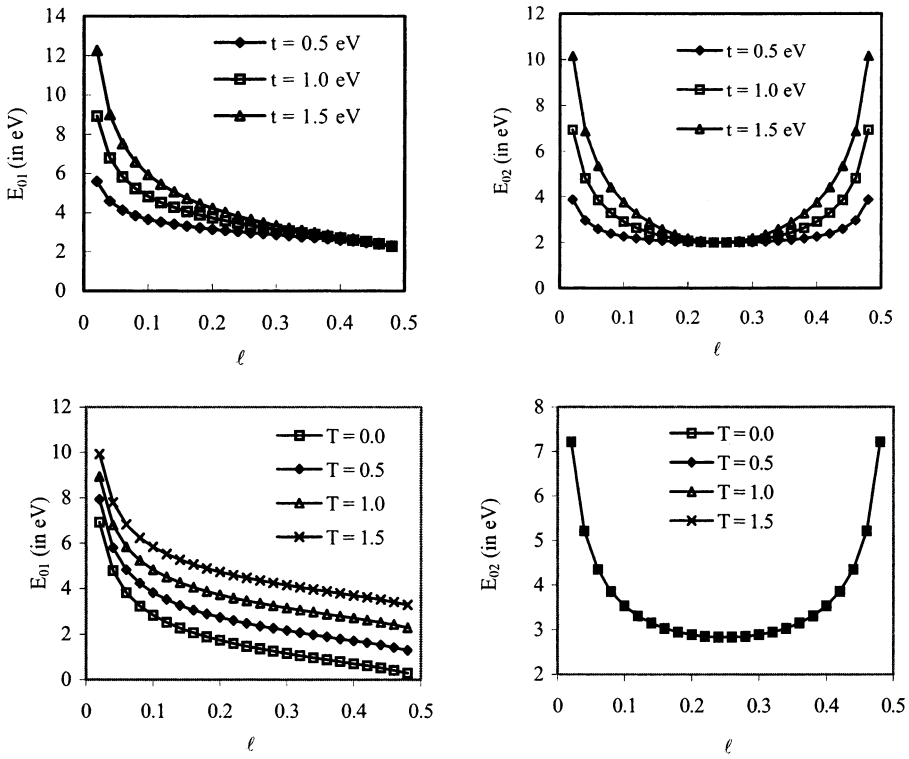

Figure 4. $E_{01} = E_1 - E_0$ (left) and $E_{02} = E_2 - E_0$ (right) as a function of ℓ for different values of t ($T = 1.0$ eV) (top) as well as for different values of T ($t = 1.0$ eV) (bottom).

integrals t and T. V is determined by the nature of D/A groups and the conjugated linkers. A detailed discussion of the structure-dependence of V for push−pull conjugated systems by Del Zoppo et al.[57] illustrates that strengthening the D/A pair favors the stabilization of the CT states and therefore decreases V, while lengthening the conjugation path makes the charge transfer from the donor to the acceptor more difficult and therefore increases V. δ approaches $\pi/2$ ($\ell = 0$) in the extreme limit of $V \gg 0$ (eq 8), indicating that the ground state is totally determined by the VB configuration. In the limit of $V \ll 0$, δ approaches 0 ($\ell = {}^1/_2$) and the ground state is completely determined by the two CT configurations in equal populations. Figure 3 shows the variation of ℓ when V ranges from −2 to +2 eV. The larger t, the slower the variations of ℓ with V. On the other hand, changing T mostly results in lateral shifts of the ℓ versus V curve. Increasing T leads to an increase in ℓ which attains a maximum in the region of $T \approx V$, whereas an increase in t is associated either with an increase ($V > T$) or a decrease ($V < T$) of ℓ. Moreover, when the transfer integral T becomes very large, ℓ tends toward ${}^1/_2$, whereas $\ell = {}^1/_4$ characterizes the limit of very large transfer integrals t.

From eqs 2−4, the energy differences between the ground and excited states read as

$$E_{01} = \frac{1}{2}(V + 3T) + \frac{1}{2}\sqrt{(V - T)^2 + 8t^2} = 2T + t\sqrt{\frac{1}{\ell} - 2} \tag{9}$$

$$E_{02} = \sqrt{(V - T)^2 + 8t^2} = \frac{t}{\sqrt{\ell(1 - 2\ell)}} \tag{10}$$

Figure 4 illustrates the variations of E_{01} and E_{02} with ℓ for different values of the T and t parameters. When V ranges from positive to negative, i.e., when the CT character increases, E_{01} decreases, whereas E_{02} drops first and then increases after reaching a minimum at $V = T$. The smallest E_{01} ($=2T$) is obtained for $V \ll 0$ and corresponds, as discussed above, to the situation where the ground state is dominated by the two CT forms ($\ell = {}^1/_2$). On the other hand, E_{02} presents a minimum for $\ell = {}^1/_4$. When fixing T, the larger t, the larger both excitation energies. Similarly, for a given t, E_{01} decreases when T becomes smaller, whereas E_{02} does not depend on T because all its dependence is included in the changes in ℓ.

The dipole moment of the VB form is negligible compared to that of either CT forms, that is, $\mu_{VB} \approx 0$. Under the Cartesian axes defined in Figure 1, the dipole moments of the two CT forms can be written as

$$\mu_{CT1} = \mu(-\sin\theta, 0, \cos\theta) \tag{11}$$

$$\mu_{CT2} = \mu(\sin\theta, 0, \cos\theta) \tag{12}$$

where μ is the absolute magnitude of the dipole moment of each CT configuration. By invoking the usual approximations of VB−CT treatments, $\langle\phi_{VB}|\hat{\mu}|\phi_{CT1}\rangle = \langle\phi_{VB}|\hat{\mu}|\phi_{CT2}\rangle = 0$ and $\langle\phi_{CT1}|\hat{\mu}|\phi_{CT2}\rangle = 0$, the permanent dipole moment as well as the transition dipole moments read:

$$\mu_0 = (0, 0, \mu\cos^2\delta\cos\theta) = (0, 0, 2\ell\mu\cos\theta) \tag{13}$$

$$\mu_1 = (0, 0, \mu\cos\theta) \tag{14}$$

$$\mu_2 = (0, 0, \mu\sin^2\delta\cos\theta) = [0, 0, (1 - 2\ell)\mu\cos\theta] \tag{15}$$

$$\mu_{01} = (-\mu\cos\delta\sin\theta, 0, 0) = (-\sqrt{2\ell}\mu\sin\theta, 0, 0) \tag{16}$$

$$\mu_{02} = \left(0, 0, \frac{1}{2}\mu\sin 2\delta\cos\theta\right) = [0, 0, \sqrt{2l(1 - 2\ell)}\mu\cos\theta] \tag{17}$$

$$\mu_{12} = (-\mu\sin\delta\sin\theta, 0, 0) = (-\sqrt{(1 - 2\ell)}\mu\sin\theta, 0, 0) \tag{18}$$

For all states, only the z component of the dipole moment is nonzero. In particular, from eq 13, the dipole moment of the ground state, μ_0, is proportional to $\cos^2\delta$ (2ℓ). Stronger D/A groups tend therefore to produce a larger dipole moment. For symmetry reasons, only three transition dipole elements, μ^x_{01}, μ^z_{02}, and μ^x_{12}, are different from zero. Within the three-state model, the total β_{xxz} response can be decomposed into two contributions, a so-called dipolar term, β^D_{xxz}, and a two-photon-like term, β^{TP}_{xxz}. From eqs 9 and 10 and 13−18, we have

$$\begin{aligned}
\beta_{xxz} &= \beta^D_{xxz} + \beta^{TP}_{xxz} \\
&= 2\frac{(\mu^x_{01})^2(\mu^z_1 - \mu^z_0)}{E_{01}{}^2} + 4\frac{\mu^x_{01}\mu^x_{12}\mu^z_{20}}{E_{01}E_{01}} \\
&= \frac{1}{2}\mu^3\sin^2 2\delta\left(\frac{1}{E_{01}{}^2} + \frac{2}{E_{01}E_{02}}\right)\sin^2\theta\cos\theta \\
&= 4\ell(1 - 2\ell)\mu^3\left(\frac{1}{E_{01}{}^2} + \frac{2}{E_{01}E_{02}}\right)\sin^2\theta\cos\theta \\
&= 4\ell(1 - 2\ell)\mu^3\left(\frac{1}{\left(2T + t\sqrt{\frac{1}{\ell} - 2}\right)^2} + \right. \\
&\qquad \left. \frac{2}{\left(2T + t\sqrt{\frac{1}{\ell} - 2}\right)\left(\frac{t}{\sqrt{\ell(1 - 2\ell)}}\right)}\right)\sin^2\theta\cos\theta
\end{aligned} \tag{19}$$

Because $\mu^z_{12} = 0$, β_{zzz} reduces to the dipolar term:

$$\begin{aligned}
\beta_{zzz} &= \beta^D_{zzz} \\
&= 6\frac{(\mu^z_{02})^2(\mu^z_2 - \mu^z_0)}{E_{02}{}^2} \\
&= -\frac{3\mu^3\sin^2 2\delta\cos 2\delta}{2E_{02}{}^2}\cos^3\theta \\
&= \frac{12\ell(1 - 2\ell)(1 - 4\ell)\mu^3}{E_{02}{}^2}\cos^3\theta \\
&= \frac{12\ell^2(1 - 2\ell)^2(1 - 4\ell)\mu^3}{t^2}\cos^3\theta
\end{aligned} \tag{20}$$

Figure 5 illustrates the variation of β^D_{xxz}, β^{TP}_{xxz}, and β^D_{zzz} as a function of ℓ for T = 1.5, 1.0, 0.5, and 0 eV using the assumptions of t = 1.0 eV and $2\theta = 120°$. In this plot as well as for Figures 6−8, we used the expression in terms of the ℓ, t, and T parameters; that is, any other quantity (such as E_{01}, ...) is expressed in terms of these three parameters. When $T \neq 0$, both β^{TP}_{xxz} and β^D_{xxz} increase with increasing ℓ until a maximum is attained and then they decrease. However, the former reaches the maximum at relatively smaller ℓ values. β^{TP}_{xxz} is smaller than β^D_{xxz} only for large value of ℓ. This inversion of the relative

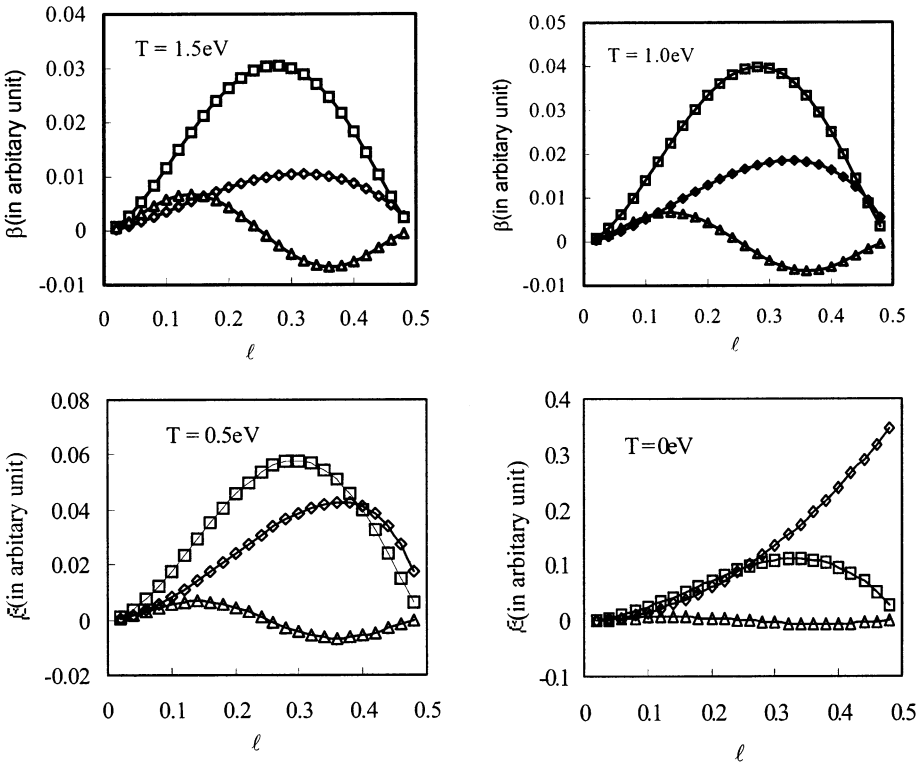

Figure 5. Comparison between the β_{xxz} and β_{zzz} versus ℓ curves for different values of T. Squares, diamonds, and triangles denote β^{TP}_{xxz}, β^{D}_{xxz}, and β^{D}_{zzz}, respectively. $t = 1.0$ eV, $2\theta = 120°$.

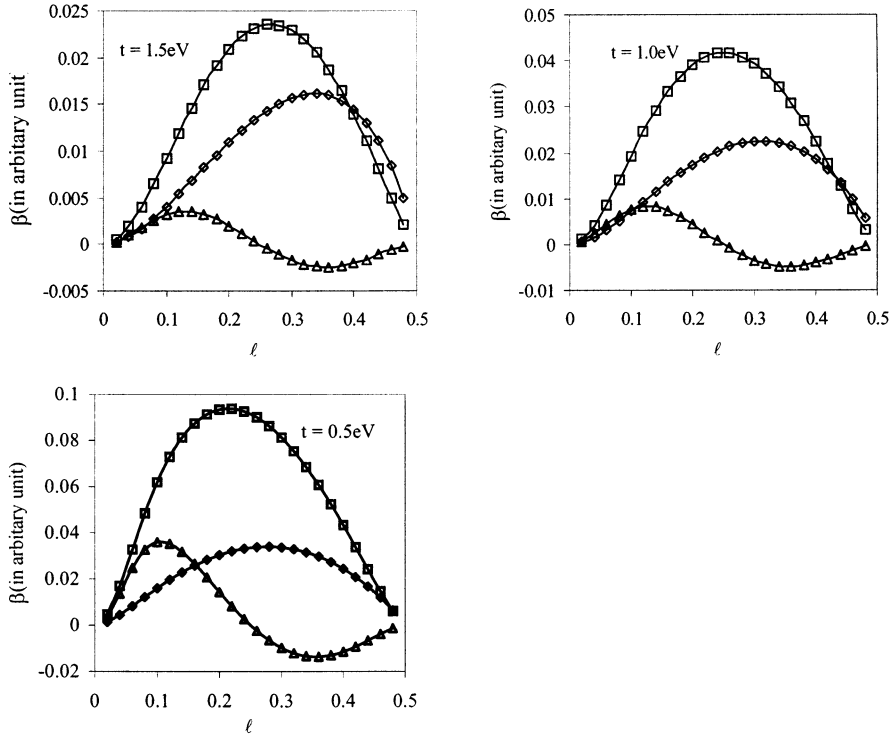

Figure 6. Comparison between the β_{xxz} and β_{zzz} versus ℓ curves for different values of t. Squares, diamonds, and triangles denote β^{TP}_{xxz}, β^{D}_{xxz}, and β^{D}_{zzz}, respectively. T = 1.0 eV, $2\theta = 120°$.

amplitudes of β^{TP}_{xxz} and β^{D}_{xxz} appears at relatively smaller ℓ values when T gets smaller. In the extreme case of $T = 0$, β^{D}_{xxz} becomes larger than β^{TP}_{xxz} for $\ell > 1/4$, whereas β^{D}_{zzz} is much smaller. The transfer integral T has a great effect on the off-diagonal components β^{D}_{xxz} and β^{TP}_{xxz} which increase when T decreases. In Barzoukas and Blanchard-Desce's treatment[42] for the D−A−A−D-like quadrupolar molecules, the coupling T is neglected as a result of the disconnection between the two D−A pairs. The situation is however different for DAD (ADA)-like quadrupolar or the guanidinium-type octupolar molecules in which all of the D−A pairs share the same acceptor (donor) and the coupling between any two CT forms cannot be ignored any longer. The situation is different for the diagonal dipolar term. Indeed, first all β^{D}_{zzz} versus ℓ curves are identical when

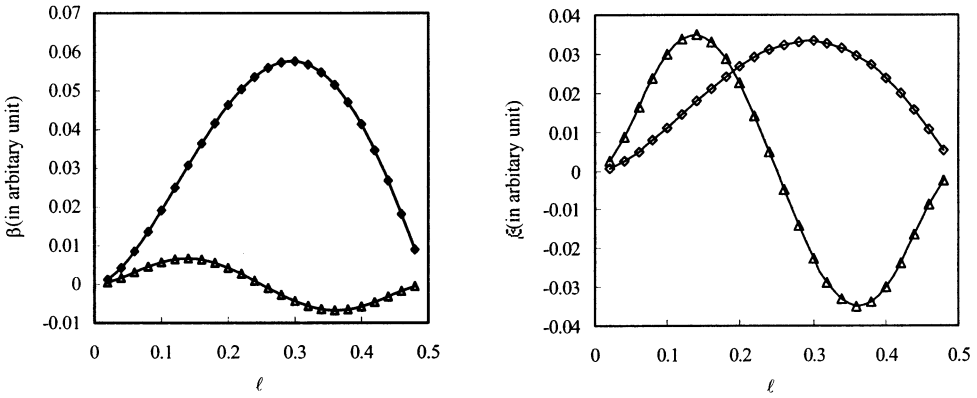

Figure 7. β_{xxz} and β_{zzz} components of Λ-shaped molecules as a function of ℓ for $T = t = 1.0$ eV and $2\theta = 120°$ (left) and $2\theta = 60°$ (right). Diamonds and triangles denote β_{xxz} and β_{zzz}, respectively.

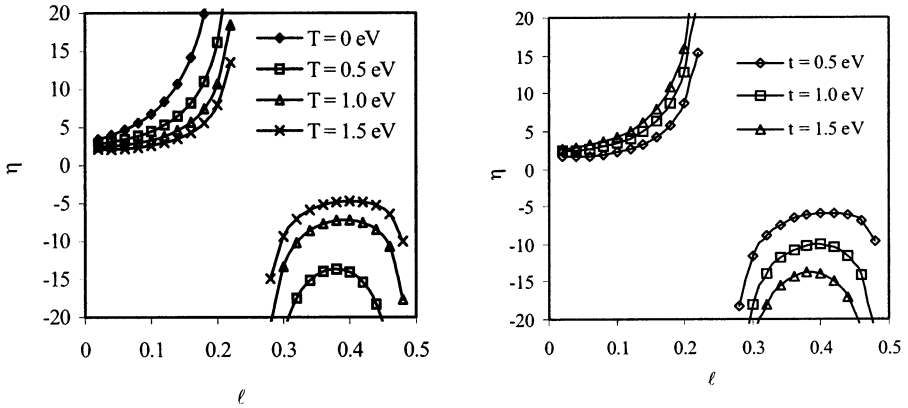

Figure 8. $\eta = \beta_{xxz}/\beta_{zzz}$ as a function of ℓ for $2\theta = 120°$ (left) and $2\theta = 60°$ (right). $t = 1.0$ eV (left), whereas $T = 1.0$ eV (right).

varying T. In addition, β^{D}_{zzz} is positive when ℓ ranges from 0 to $^1/_4$ (δ from $\pi/2$ to $\pi/4$) and becomes negative when $\ell = {}^1/_4 - {}^1/_2$. Positive and negative extrema are observed for $\ell = 0.137$ and 0.363, respectively. Consequently, the β^{D}_{zzz} versus ℓ curves are similar in shape with these of one-dimensional D/A systems.[30,32] Nevertheless, they differ in several ways: (i) the coupling between the two CT states (T) modifies (through ℓ) E_{02} as well as the dipole moments and (ii) the coupling between the VB state and the two CT states increases the gap. Indeed, for a one-dimensional D/A system, the square of the gap, as predicted by the VB−CT model, amounts to $V^2 + 4t^2$,[38] whereas for Λ-shaped molecules with $T = 0$, it attains $V^2 + 8t^2$. In addition, β^{D}_{zzz} is modulated by the angle between the two D/A axes. Figure 6 illustrates the variations of β^{D}_{xxz}, β^{TP}_{xxz}, and β^{D}_{zzz} with ℓ for $t = 1.5$, 1.0, and 0.5 eV using the assumptions of $T = 1.0$ eV and $2\theta = 120°$. When t increases, all β components decrease, and the relative importance of β^{D}_{zzz} with respect to both β_{xxz} components decreases while the $\beta^{D}_{xxz}/\beta^{TP}_{xxz}$ ratio increases.

Figure 7 compares the diagonal and off-diagonal β components for $T = t = 1.0$ eV as a function of 2θ (= 120° or 60°). Following eqs 19 and 20, β_{zzz} and β_{xxz} exhibit different behaviors as a function of 2θ. With 2θ ranging from 0° to 180°, β_{zzz} drops monotonically, whereas β_{xxz} increases first, attains a maximum for $2\theta = 109.47°$, and then drops. From eqs 19 and 20, the ratio between the off-diagonal and diagonal components reads

$$\eta = \frac{\beta_{xxz}}{\beta_{zzz}} = \frac{1}{3}\frac{tg^2\theta}{1-4\ell}\left[2\frac{E_{02}}{E_{01}} + \left(\frac{E_{02}}{E_{01}}\right)^2\right] \qquad (21)$$

The amplitude of η can be analyzed by considering three contributions: the θ factor, the $1/(1 - 4\ell)$ term and the E_{02}/E_{01} ratio although the later two are intertwined. The $tg^2\theta$ term is equal to unity for $2\theta = 90°$, smaller than unity for $2\theta < 90°$ and larger than unity for the other cases ($0° < 2\theta < 180°$). In particular for $2\theta = 60°$, $tg^2\theta = {}^1/_3$, whereas for $2\theta = 120°$, $tg^2\theta = 3$. Within the domain of variation of ℓ, [0, $^1/_2$], the $1/(1 - 4\ell)$ factor is, in magnitude, always larger than unity and becomes very large for $\ell \approx {}^1/_4$. This factor is positive for $\ell < {}^1/_4$ but negative for $\ell > {}^1/_4$. The third term, $[2E_{02}/E_{01} + (E_{02}/E_{01})^2]$, is more complex to analyze. It is larger than 3 when $E_{02} > E_{01}$ or equivalently when $\ell > T^2/(t^2 + 2T^2)$ which implies that t should be large enough with respect to T. Moreover, for $t \geq T/4$, it can be shown that $[2E_{02}/E_{01} + (E_{02}/E_{01})^2] > 1$. Thus, for $2\theta = 120°$, η is expected to be often larger than unity. This corroborates why, for $2\theta = 120°$, the total off-diagonal component, $\beta_{xxz} = \beta^{D}_{xxz} + \beta^{TP}_{xxz}$, is always larger than β_{zzz}. On the other hand, the diagonal contribution increases when the angle between the two D/A arms becomes smaller. Figure 8 illustrates the variation of η with ℓ for $2\theta = 120°$ and different values of the T and t. In the range of $\ell = 0 - {}^1/_4$, η increases with increasing ℓ, and larger η values correspond to smaller T and larger t. Because $\beta_{zzz} = 0$ for $\ell = {}^1/_4$, η displays an asymptotic behavior in that region. When ℓ goes from $^1/_4$ to $^1/_2$, the absolute value of η drops first and then increases after reaching a minimum.

As a consequence, it turns out feasible to modulate the CT character and the 2θ angle in order to design chromophores with specific η values while keeping large second-order NLO responses. Moreover, both DAD- and ADA-type molecules can be characterized by the VB-2CT model, the only difference between these two classes of compounds is the sign or direction of μ and consequently, of the different β components that are proportional to the third power of μ. For simplicity, μ is chosen

positive so that negative β values correspond to the situation where μ and β are antiparallel. In the next section, the VB-2CT observations are used to rationalize the ab initio and semiempirical results of section 3.

5. Further Discussions and Conclusions

The VB-2CT structure−property relationships for the β-tensor components of DAD- and ADA-types Λ-shaped molecules can be summarized as follows:

(i) β_{xxz} is always positive (β parallel to μ), and its α dependence presents one maximum, whereas β_{zzz} is positive for weak D/A pair but negative for strong ones, and β_{zzz} presents two extrema (for α values close to $^1/_8$ and $^3/_8$). β_{zzz} decreases monotonically with 2θ, whereas β_{xxz} increases, attains a maximum at $2\theta = 109.47°$, and then decreases.

(ii) β_{xxz} is larger than β_{zzz} if the angle between the two D/A branches is larger than 120° and $t \geq T/4$. This also happens for smaller values of 2θ provided t and/or $1/(1 - 4\alpha)$ are large enough. On the other hand, when the angle is small, β_{zzz} can be larger than β_{xxz}, especially around the intermediate values of α that correspond to the extrema of β_{zzz} versus α.

(iii) Larger $\beta_z = \beta_{xxz} + \beta_{yyz} + \beta_{zzz} \approx \beta_{xxz} + \beta_{zzz}$ can be achieved when the two components are positive, in particular when $\alpha \approx {}^1/_8$, whereas β_z can be small for $\alpha \approx {}^3/_8$. As a consequence, the elaboration of structure−property relationships and the subsequent design of NLO chromophores for solid state applications which would be solely based on EFISH (for electric field-induced second harmonic generation) measurements can be misleading in cases where β_{xxz} and β_{zzz} are large and cancel each other.

(iv) For a fixed value of α, increasing T induces a diminution of β_{xxz}, does not affect β_{zzz}, and therefore decreases η whereas increasing t is mostly associated with a reduction of all β components and an increase in η.

The combined VB-2CT and ab initio study has demonstrated that both electronic and geometric factors influence the magnitude of β_{xxz} and β_{zzz} as well as of their ratio η. In simple cases such as the comparison between the molecules of the B, C, F, G, H, and I groups, the geometric factor explains why η is small (C, G, and H groups) or large (B, F, and I groups). The general situation, where the electronic factors associated with the interactions between the donor and acceptor moieties play an important role on the sign and magnitude of the β components, is however often more complicated. Strong D/A pairs often yield large dipole moments for the CT states and are therefore in favor of large ground-state dipole moments and first hyperpolarizability tensor components. This explains, for instance, the increase in μ_z and β_{xxz} when going from the J (R = CN) to K (R = NO_2) molecules. However, very powerful D/A pairs do no mean very large β values. Indeed, as predicted by the VB-2CT model, there are optimal α values to maximize β_{xxz} and β_{zzz}, and they do not coincide. Moreover, the real molecules usually span a narrow range of α belonging to the [0, $^1/_4$] interval, and the examples studied in the present contribution do not give a full picture of β variations with different α. Most β_{zzz} values reported in Table 2 are positive or, if negative, small. The same is true for Table 1 for the cases where σ-inductive effects have a minimal importance. In a few cases, the β_{xxz} and β_{zzz} components have opposite signs. For the molecules of the group A, this can be attributed to the strong D/A interactions, which lead to large α values and then, from Figures 3−5, to opposite signs of β_{xxz} and β_{zzz}. Although strong donors and/or strong acceptors exist in other molecules (like these of the E group), the coupling between the donor and the acceptor is diluted because of the conjugated linker,[57] unlike the case in A1 and A2 in which the donors connect directly with the acceptors. Moreover, for the molecules of the F and I groups, increasing the donor character by substituting the OH by the NH_2 group increases β_{xxz} but leads to a sign change for β_{zzz}. By going from the I to H species, the distance between the D and A moieties increases, whereas the 2θ angle is reduced by a factor of almost 2. After factorizing out the θ dependence, i.e., by dividing β_{xxz} and β_{zzz} by $\sin^2\theta \cos\theta$ and $\cos^3\theta$, respectively, the H compounds present larger β_{xxz} and β_{zzz} values than the I compounds, in agreement with larger values of t and/or T in I than H. Indeed, for given 2θ values, increasing t and T leads to a decrease of β (Figures 5 and 6). A similar reasoning applies to the difference in β_{xxz} between G1 and H1 (G2 and H2), whereas for β_{zzz}, the variations are much smaller.

In the VB-2CT treatment, one ground-state S_0 and two excited states S_1 and S_2 are involved in the sum-over-state analysis. Experimentally,[17,23] two low-lying excited states have also been detected and their splitting associated with the coupling between them. As shown by eqs 16 and 17 (as well as 9 and 10), the relative magnitude of the transition dipole moments and oscillator strengths are not only dictated by the 2θ angle but also by the CT character and coupling term. Furthermore, like in ref 17, the second transition is polarized parallel to the CT axis, whereas the first is polarized perpendicular to it. As a consequence, β_{xxz} contains contributions from both S_1 and S_2, whereas β_{zzz} depends only on S_2. Only a two-level term contributes to β_{zzz}, whereas both two-level (dipolar) and three-level (two-photon like) terms contribute to β_{xxz}. In addition, as can be seen in Figure 5, the contribution to β_{xxz} from three-level terms is larger than that from two-level terms except in case with T approaching zero.

In summary, the VB-2CT model turns out to be a simple but useful means to qualitatively describe the electronic component of the NLO properties of Λ-shaped molecules in addition to dipolar, quadrupolar, ..., push−pull systems. For the Λ-shaped molecules with DAD- or ADA-patterns, it gives predictions agreeing well with quantum chemical calculations of the first hyperpolarizability. It further shows that by building compounds with a suitable angle between the D/A axes and by tuning the CT character, specific ratios between the off-diagonal and diagonal β-tensor components can be achieved while maintaining large NLO responses. By considering this property with their high thermal stability and the nonlinearity-transparence tradeoff, it appears that Λ-shaped molecules are promising candidates to build phase-matchable SHG crystals.

Acknowledgment. M.Y. and B.C. thank the Belgian National Fund for Scientific Research (FNRS) for their postdoctoral grant and Senior Research Associate position, respectively. Calculations were performed on the IBM SP2 of the Namur Scientific Computing Facility (Namur-SCF) for which the authors gratefully acknowledge the financial support of the FNRS-FRFC and the "Loterie Nationale" for the convention No. 2.4519.97 as well as on a cluster of PC acquired thanks to a "crédit aux chercheurs" of the FNRS. The authors thank partial support from the Belgian Federal Interuniversity Attraction Pole on "Supramolecular Chemistry and Supramolecular Catalysis" (IUAP No. P5-03).

References and Notes

(1) Prasad, P. N.; William, D. J. *Introduction to Nonlinear Optical Effects in Molecules and Polymers*; John Wiley: New York, 1991.

(2) Kanis, D. R.; Ratner, M. A.; Marks, T. J. *Chem. Rev.* **1994**, *94*, 195.

(3) Bosshard, Ch.; Sutter, K.; Prêtre, Ph.; Hulliger, J.; Flörsheimer, M.; Kaatz, P.; Günter, P. *Organic Nonlinear Optical Materials* in *Advances in Nonlinear Optics*; Garito, A. F., Kajzar, F., Ed.; Gordon & Breach: Basel, 1995.

(4) Kirtman, B.; Champagne, B. *Int. Rev. Phys. Chem.* **1997**, *16*, 389.

(5) Verbiest, T.; Houbrechts, M.; Kauranen, M.; Clays, K.; Persoons, A. *J. Mater, Chem.* **1997**, *7*, 2175.

(6) Champagne, B.; Kirtman, B., in *Handbook of Advanced electronic and Photonic Materials and Devices*; Nalwa, H. S., Ed.; Academic Press: 2001; Vol. 9, Chapter 2, p 63. Champagne, B. *Élaboration de methodes de chimie quantique pour l'évaluation des hyperpolarisabilités vibrationnelles − Conséquences pour l'optique non linéaire*; Presses Universitaires de Namur: Namur, Belgique, 2001.

(7) Zyss, J.; Ledoux, I.; Bertault, K.; Toupet, E. *Chem. Phys*. **1991**, *150*, 125.

(8) Marder, R.; Kippelen, B.; Jen, A. K.-Y.; Peyghambarian, N. *Nature* **1997**, *388*, 845.

(9) Yamamoto, H.; Katogi, S.; Watanabe, T.; Sato, H.; Miyata, S.; Hosomi, T. *Appl. Phys. Lett.* **1992**, *60*, 935.

(10) Kuo, W.-J.; Hsiue, G.-H.; Jeng, R.-J. *Macromolecules* **2001**, *34*, 2373.

(11) Zyss, J.; Oudar, J. L. *Phys. Rev. A* **1982**, *26*, 2028.

(12) See, for example: Champagne, B.; Bishop, D. M. *Adv. Chem. Phys.* **2003**, *726*, 47.

(13) Wong, M. S.; Bosshard, C.; Pan, F.; Günter, P. *Adv. Mater*. **1996**, *8*, 677.

(14) Brédas, J. L.; Meyers, F.; Pierce, B. M.; Zyss, J. *J. Am. Chem. Soc*. **1992**, *114*, 4928. Zyss, J.; Ledoux, I. *Chem. Rev*. **1994**, *94*, 77.

(15) Miyata, S.; Sasabe, H. *Poled Polymers and Their Applications to SHG and EO Devices*; Gordon and Breach Science: Australia, 1997.

(16) Wortmann, R.; Krämer, P.; Glania, C.; Lebus, S.; Detzer, N. *Chem. Phys.* **1993**, *173*, 99. Rao, V. P.; Jen, A. K. Y.; Cai, Y. *Chem. Commun.* **1996**, 1237.

(17) Moylan, C. R.; Ermer, S.; Lovejoy, S. M.; McComb, I.-H.; Leung, D. S.; Wortmann, R.; Krdmer, P.; Twieg, R. J. *J. Am. Chem. Soc*. **1996**, *118*, 12950.

(18) Yakimanski, A. V.; Kolb, U.; Matveeva, G. N.; Voigt-Martin, I.; Tenkovtsev, A. V. *Acta Crystallogr*. **1997**, *A53*, 603.

(19) Wortmann, R.; Glania, C.; Krämer, P.; Matschiner, R.; Wolff, J. J.; Kraft, S.; Treptow, B.; Barbu, E.; Daniela, L.; Görlitz, G. *Chem. Eur. J.* **1997**, *3*, 1765.

(20) Wolff, J. J.; Lngle, D.; Hillenbrand, D.; Wortmann, R.; Matschiner, R.; Glania, C.; Krämer, P. *Adv. Mater.* **1997**, *9*, 138.

(21) Van Elshocht, S.; Verbiest, T.; Kauranen, M.; Ma, L.; Cheng, H.; Musick, K.; Pu, L.; Persoons, A. *Chem. Phys. Lett.* **1999**, *309*, 315.

(22) Liu, Y. J.; Liu, Y.; Zhang, D. J.; Hu, H. Q.; Liu, C. B. *J. Mol. Struct.* **2001**, *570*, 43.

(23) Ostroverkhov, V.; Petschek, R. G.; Singer, K. D.; Twieg, R. J. *Chem. Phys. Lett.* **2001**, *340*, 109.

(24) Averseng, F.; Lacroix, P. G.; Malfant, I.; Lenoble, G.; Cassoux, P.; Nakatani, K.; Maltey-Fanton, I.; Delaire, J. A.; Aukauloo, A. *Chem. Mater*. **1999**, *11*, 995.

(25) Le Bozec, H.; Renouard, T. *Eur. J. Inorg. Chem.* **2000**, 229.

(26) Di Bella, S.; Fragalà, L.; Ledoux, I.; Zyss, J. *Chem. Eur. J.* **2001**, *7*, 3738.

(27) Moylan, C. R.; Twieg, R. J.; Lee, V. Y.; Swanson, S. A.; Betterton, K. M.; Miller, R. D. *J. Am. Chem. Soc.* **1993**, *115*, 12599.

(28) Mulliken, R. S. *J. Am. Chem. Soc*. **1952**, *74*, 811.

(29) Chen, G.; Lu, D.; Goddard, W. A., III. *J. Chem. Phys*. **1994**, *101*, 5860.

(30) Lu, D.; Chen, G.; Perry, J. W.; Goddard, W. A., III. *J. Am. Chem. Soc*. **1994**, *116*, 10679.

(31) Castiglioni, C.; Del Zoppo, M.; Zerbi, G. *Phys. Rev. B.* **1996**, *53*, 13319.

(32) Barzoukas, M.; Runser, C.; Fort, A.; Blanchard-Desce, M. *Chem. Phys. Lett*. **1996**, *257*, 531.

(33) Blanchard-Desce, M.; Barzoukas, M. *J. Opt. Soc. Am. B* **1998**, *15*, 302.

(34) Bishop, D. M.; Kirtman, B. *Phys. Rev. B*, **1996**, *56*, 2273. Castiglioni, C.; Del Zoppo, M.; Zerbi, G. *Phys. Rev. B.* **1996**, *56*, 2275.

(35) Kim, H.-S.; Cho, M.; Jeon, S.-J. *J. Chem. Phys*. **1997**, *107*, 1936.

(36) Cho, M. *J. Phys. Chem. A* **1998**, *102*, 703.

(37) Painelli, A. *Chem. Phys. Lett.* **1998**, *285*, 352.

(38) Bishop, D. M.; Champagne, B.; Kirtman, B. *J. Chem. Phys*. **1998**, *109*, 9987.

(39) Cho, M.; Kim, H.-S.; Jeon, S.-J. *J. Chem. Phys*. **1998**, *108*, 7114.

(40) Lee, Y.-K.; Jeon, S.-J.; Cho, M. *J. Am. Chem. Soc*. **1998**, *120*, 10921.

(41) Hahn, S.; Kim, D.; Cho, M. *J. Phys. Chem. B* **1999**, *103*, 8221.

(42) Barzoukas, M.; Blanchard-Desce, M. *J. Chem. Phys.* **2000**, *113*, 3951.

(43) Cho, M.; Am, S.-Y.; Lee, H.; Ledoux, I.; Zyss, J. *J. Chem. Phys.* **2002**, *116*, 9165.

(44) Exner, O. In *Correlation Analysis in Chemistry*; Chapman, N. B., Shorter, J., Eds.; Plenum Press: New York, 1978; Chapter 10, p 439.

(45) Dewar, M. J. S.; Zoebisch, E. G.; Healy, E. F.; Stewart, J. J. P. *J. Am. Chem. Soc.* **1985**, *107*, 3902.

(46) Cohen, H. D.; Roothaan, C. C. J. *J. Chem. Phys.* **1965**, *43*, S34.

(47) Jacquemin, D.; Champagne, B.; André, J. M. *Int. J. Quantum. Chem.* **1997**, *65*, 679.

(48) Davis, P. J.; Rabinowitz, P. *Numerical Integration*; Blaisdell Publishing Company: London, 1967; p 166.

(49) Jacquemin, D.; Champagne, B.; Hättig, C. *Chem. Phys. Lett*. **2000**, *319*, 327.

(50) Jacquemin, D.; Champagne, B.; Perpète, E. A.; Luis, J. M.; Kirtman, B. *J. Phys. Chem. A* **2001**, *105*, 9748.

(51) Frisch, M. J.; Trucks, G. W.; Schlegel, H. B.; Scuseria, G. E.; Robb, M. A.; Cheeseman, J. R.; Zakrzewski, V. G.; Montgomery, J. A., Jr.; Stratmann, R. E.; Burant, J. C.; Dapprich, S.; Millam, J. M.; Daniels, A. D.; Kudin, K. N.; Strain, M. C.; Farkas, O.; Tomasi, J.; Barone, V.; Cossi, M.; Cammi, R.; Mennucci, B.; Pomelli, C.; Adamo, C.; Clifford, S.; Ochterski, J.; Petersson, G. A.; Ayala, P. Y.; Cui, Q.; Morokuma, K.; Malick, D. K.; Rabuck, A. D.; Raghavachari, K.; Foresman, J. B.; Cioslowski, J.; Ortiz, J. V.; Stefanov, B. B.; Liu, G.; Liashenko, A.; Piskorz, P.; Komaromi, I.; Gomperts, R.; Martin, R. L.; Fox, D. J.; Keith, T.; Al-Laham, M. A.; Peng, C. Y.; Nanayakkara, A.; Gonzalez, C.; Challacombe, M.; Gill, P. M. W.; Johnson, B. G.; Chen, W.; Wong, M. W.; Andres, J. L.; Head-Gordon, M.; Replogle, E. S.; Pople, J. A. *Gaussian 98*, revision A.11; Gaussian, Inc.: Pittsburgh, PA, 1998.

(52) Stewart, J. J. P. *MOPAC*, Quantum Chemistry Program Exchange, #455.

(53) Korambath, P.; Kurtz, H. A. In *Nonlinear Optical Materials, Theory and Modeling*; Karna, S. P., Yeates, A. T., Eds.; ACS Symposium Series;l American Chemical Society: Washington, DC, 1996; Vol. 628, p 133.

(54) Champagne, B. *Int. J. Quantum Chem.* **1997**, *65*, 689.

(55) Ermer, S.; Girton, D. G.; Leung, D. S.; Lovejoy, S. M.; Valley, J. F.; Van Eck, T. E.; Cheng, L.-T. *Nonlinear Opt.* **1995**, *9*, 259.

(56) Wolff, J. J.; Wortmann, R. *Adv. Phys. Org. Chem.* **1999**, *32*, 121.

(57) Del Zoppo, M.; Castiglioni, C.; Gerola, V.; Zuliani, P.; Zerbi, G. *J. Opt. Soc. Am. B* **1998**, *15*, 308.

(58) Jacquemin, D.; Beljonne, D.; Champagne, B.; Geskin, V.; Brédas, J. L.; André, J. M. *J. Chem. Phys.* **2001**, *115*, 6766.